

H-PDLC based waveform controllable optical choppers for FDMF microscopy

Jihong Zheng,^{1,*} Guoqiang Sun,¹ Yanmeng Jiang,¹ Tingting Wang,¹ Aiqing Huang,¹ Yunbo Zhang,¹ Pingyu Tang,¹ Songlin Zhuang,¹ Yanjun Liu,² and Stuart Yin³

¹College of Optics and Electron Information Engineering, University of Shanghai for Science and Technology, Shanghai 200093, China

²Department of Engineering Science and Mechanics, The Pennsylvania State University, Pennsylvania 16802, USA

³Department of Electrical Engineering, The Pennsylvania State University, Pennsylvania 16802, USA

*jihongzheng2002@yahoo.com.cn

Abstract: An electrically waveform controllable optical chopper based on holographic polymer dispersed liquid crystal grating (H-PDLC) is presented in this paper. The theoretical analyses and experimental results show that the proposed optical chopper has following merits: (1) controllable waveform, (2) no mechanical motion induced vibrational noise, and (3) multiple-channel integration capability. The application of this unique electrically controllable optical chopper to frequency division multiplexed fluorescent microscopy is also addressed in this paper, which has the potential to increase the channel capacity, the stability and the reliability. This will be beneficial to the parallel detection, especially for dynamic studies of living biological samples.

©2011 Optical Society of America

OCIS codes: (230.2090) Electro-optical devices; (110.0180) Microscopy; (090.2890) Holographic optical elements; (110.2970) Image detection systems.

References and links

1. F. Wu, X. Q. Zhang, J. Y. Cheung, K. B. Shi, Z. W. Liu, C. Luo, S. Yin, and P. Ruffin, "Frequency division multiplexed multichannel high-speed fluorescence confocal microscope," *Biophys. J.* **91**(6), 2290–2296 (2006).
 2. J. Pawley, *Handbook of Biological Confocal Microscopy* (Plenum Press, 1989).
 3. S. Yin, G. Lu, J. Zhang, F. T. S. Yu, and J. N. Mait, "Kinoform-based Nipkow disk for a confocal microscope," *Appl. Opt.* **34**(25), 5695–5698 (1995).
 4. T. Tanaami, S. Otsuki, N. Tomosada, Y. Kosugi, M. Shimizu, and H. Ishida, "High-speed 1-frame/ms scanning confocal microscope with a microlens and Nipkow disks," *Appl. Opt.* **41**(22), 4704–4708 (2002).
 5. K. Fujita, O. Nakanura, T. Kaneko, and M. Oyamada, "Confocal multipoint multiphoton excitation microscope with microlens and pinhole arrays," *Opt. Commun.* **174**(1–4), 7–12 (2000).
 6. A. Deniset-Besseau, S. Lévêque-Fort, M. P. Fontaine-Aupart, G. Roger, and P. Georges, "Three-dimensional time-resolved fluorescence imaging by multifocal multiphoton microscopy for a photosensitizer study in living cells," *Appl. Opt.* **46**(33), 8045–8051 (2007).
 7. S. H. Jiang, and J. Walker, "Differential high-speed digital micromirror device based fluorescence speckle confocal microscopy," *Appl. Opt.* **49**(3), 497–504 (2010).
 8. K. B. Shi, S. H. Nam, P. Li, S. Yin, and Z. Liu, "Wavelength division multiplexed confocal microscopy using supercontinuum," *Opt. Commun.* **263**(2), 156–162 (2006).
 9. L. Fu, X. S. Gan, and M. Gu, "Characterization of gradient-index lens-fiber spacing toward applications in two-photon fluorescence endoscopy," *Appl. Opt.* **44**(34), 7270–7274 (2005).
 10. H. Kikuchi, T. Fujii, M. Kawakita, Y. Hirano, H. Fujikake, F. Sato, and K. Takizawa, "High-definition imaging system based on spatial light modulators with light-scattering mode," *Appl. Opt.* **43**(1), 132–142 (2004).
 11. L. H. Domash, G. P. Crawford, and A. C. Ashmead, "Holographic PDLC for Photonic Applications," *Proc. SPIE* **4107**, 46–58 (2000).
 12. R. L. Sutherland, L. V. Natarajan, V. P. Tondiglia, and T. J. Bunning, "Bragg gratings in an acrylate polymer consisting of periodic polymer-dispersed liquid-crystal planes," *Chem. Mater.* **5**(10), 1533–1538 (1993).
 13. Y. J. Liu, and X. W. Sun, "Holographic polymer-dispersed liquid crystals: materials, formation, and applications," *Adv. Optoelectron.* **2008**, 1–53 (2008).
 14. N. S. Claxton, T. J. Fellers, and M. W. Davidson, "Laser scanning confocal microscopy", www.olympusfluoview.com/theory/LSCMIntro.pdf, (2010).
-

1. Introduction

It is well known that optical choppers are very useful for many applications. In addition to the traditional usage of modulating the light beam for increasing the detection signal-to-noise ratio of an optical system, recently, it has also been used to realize the frequency division multiplexing operation [1].

Since the middle of 1980's, fluorescence confocal microscopy has become an effective tool to detect the fluorescent biological cells [2]. In order to improve the scanning speed and spatial resolution of confocal microscopy, many techniques have been put forward and fulfilled within the confocal microscopy system, such as adopting Nipkow disk, using microlens arrays or DMD, taking optical fiber bundle, using supercontinuum laser source etc [3–9]. However, these existing techniques and methods are still insufficient for real-time biological detection in living cells. Recently, a new multi-channel parallel detection microscopic technique, the frequency-division multiplexed fluorescent (FDMF) confocal microscopy system was demonstrated [1]. The FDMF microscopy can distinguish fluorescent emissions from multiple points via different carrier frequencies, which enables high speed parallel detection capability.

A key device in FDMF microscopic system is an optical chopper. In addition to using conventional mechanical choppers [1], other kinds of light modulation techniques and devices such as the pure liquid crystal based spatial light modulators (SLMs) and electro-optic Pockel's cell may also be employed in a FDMF system. Although, in comparison to mechanical choppers, these alternative approaches have the advantages of no-mechanical motion induced vibrational noise, they also suffer some limitations. For example, the liquid crystal based SLM is a polarization-dependent device and has a limited response time (> 4 ms) [10]. The electro-optical Pockels' modulator needs a relatively high driving voltage (> 1 kV) although it offers a faster switching speed, which may not be acceptable in some systems.

In order to overcome limitations of existing optical chopper technologies, in this paper, a new kind of optical chopper based on holographic polymer dispersed liquid crystal (H-PDLC) grating is investigated. Please note that although H-PDLC based optical switch has been reported previously [11], the requirements and usage of optical switch and optical chopper is different. Only binary modulation is needed in optical switch. However, to optimize the performance, more advanced modulation schemes can be employed in the application of optical chopper. For example, by adding different modulation waveforms (such as square, triangle, sawtooth, sinusoidal) and changing duty cycles, we can increase the number of multiplexed channels in a FDMF microscopic system. In this case, not only the fundamental carrier frequency but also the shape of the waveform can be used to distinguish different modulated channels.

The major advantages of employing H-PDLC grating for the application of optical choppers are: (1) no mechanical motion induced vibrational noise, (2) polarization-independent operation, (3) waveform controllable and adjustable capability, (4) high convenience for multiple channel integration, and (5) small footprint and low power consumption. These advantages will eventually bring the FDMF microscopy with more integrated architecture, higher reliability and temporal resolution.

The organization of the paper is as follows: Section 2 introduces the fabrication method and working principle of an optical chopper based on H-PDLC gratings. Section 3 illustrates the results of waveform controllable optical choppers, including square waveform, triangular waveform, sawtooth waveform, sinusoidal waveform, as well as different duty cycles. Section 4 presents how to realize multiple channel modulation with optical choppers. Finally, for the purpose of illustration, the application of H-PDLC grating based optical chopper to FDMF microscopy is addressed in Section 5.

2. Fabrication method and working principle of electrically controlled optical chopper based on H-PDLC gratings

As aforementioned, switchable holographic polymer dispersed liquid crystal (H-PDLC) has been previously studied and used for the applications such as optical switches [12,13]. The basic working principle of H-PDLC based optical chopper is similar to the optical switch, as illustrated in Fig. 1. Without applying an electrical field, the H-PDLC gratings diffract the incident laser at the Bragg angle, while under a suitable external field, the orientation of LC droplets will be reorientated along the electrical field direction. If the ordinary refractive index of LC equals to that of polymer bonder, the grating will be erased and the incident light will go through the cell without the diffraction. If a periodical interval external electrical field is applied on the H-PDLC grating, the optical chopper function can be realized.

To fabricate the H-PDLC grating, a H-PDLC sample was firstly prepared by mixing the liquid crystal, TE300 (Tsing-Hua Yawang), prepolymer (EB8301,UCB), crosslinking monomer, N-vinylpyrrolidone (NVP) (Sigma-Aldrich), photoinitiator, Rose Bengal (RB) (Sigma-Aldrich), coinitiator, N-phenylglycine (NPG) (Sigma-Aldrich), and surfactant, S-271 (ChemService). These chemical materials were mechanically blended according to the appropriate weight ratio and stirred in an ultrasonic cleaner to form a homogeneous mixture in dark condition. After that, the syrup was sandwiched within two pieces of ITO glasses, and then subjected to the holographic exposure system. The spatial frequencies of H-PDLC gratings in our experiments vary from 600 lines/mm to 1200 lines/mm.

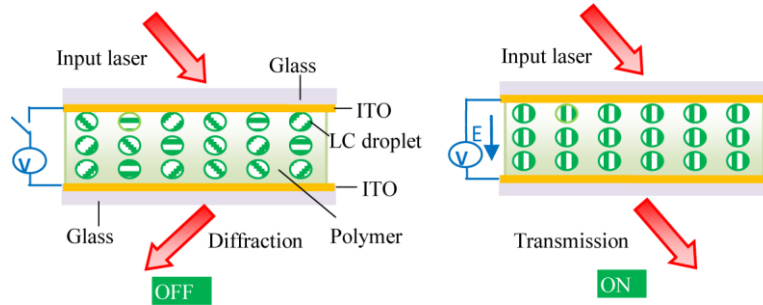


Fig. 1. An illustration of basic principle of H-PDLC chopper.

3. Waveform controllable optical choppers with electrically controlled H-PDLC gratings

To generate the optical chopping function, a periodical driving power was designed for H-PDLC gratings. Unlike conventional mechanical chopper, the waveform of modulated optical beam can be conveniently controlled by using different electrical driving signals with different profiles. For the purpose of illustrations, several kinds of waveforms, including square, triangle, sawtooth, and sinusoidal waveforms were experimentally generated.

Figure 2 shows the results of square waveform modulation of H-PDLC chopper. The amplitude of voltage, carrying frequencies and the duty ratio can be adjusted through a parallel-communication programming control system. Figure 2(a)–2(c) show the results of the H-PDLC choppers that are working at 50Hz, 100Hz, and 200Hz individually. The different duty ratio such as 1:3 at 50Hz, 1:4 and 4:1 at 200Hz are represented in Fig. 2(d)–2(f) separately. On the oscilloscope screen, the lower blue curve indicates the optical intensity modulation while the upper yellow curve shows the electrical signals that applied on the H-PDLC choppers. Although the theoretical maximum value of a pure phase grating is 100%, in our experiments, the practical maximum efficiency of H-PDLC grating is tested as 86.5% and most samples have the efficiency ranging from 40% to 70%. All of the above experiments were conducted using a 902 lines/mm H-PDLC grating sample with the tested maximum diffraction efficiency of 60.3%. The switch “ON” time and “OFF” time was tested as $\tau_{on} = 100\text{--}200\ \mu\text{s}$, $\tau_{off} = 300\text{--}400\ \mu\text{s}$. The H-PDLC cell with such diffraction efficiency is enough

to observe the obvious chopping action due to the direct part can be easily filtered by data processing.

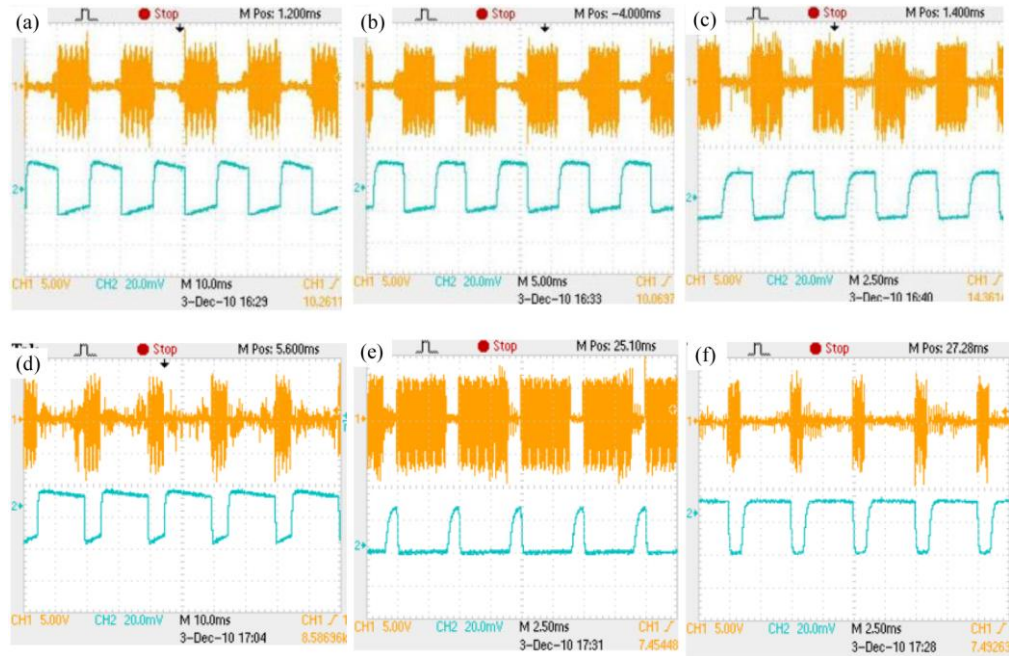


Fig. 2. H-PDLC chopper with square waveform is working with vary frequencies and different duty ratio; (a) 50Hz 1:3; (b) 100Hz 1:1; (c) 200Hz 1:1; (d) 50Hz 1:3; (e) 200Hz 4:1; (f) 200Hz 1:4.

Figure 3 shows the results of triangular waveform modulation of H-PDLC chopper. Figure 3(a)–3(c) represent the triangular waveform modulation with the variable frequencies of 27Hz, 40Hz and 100Hz respectively. Figure 3(d) was tested using the diffraction beam intensity thus it is reserved as compared with the previous three images. On the oscilloscope screen, the upper curve indicates the electrical signals while the lower curves show the optical intensity modulation.

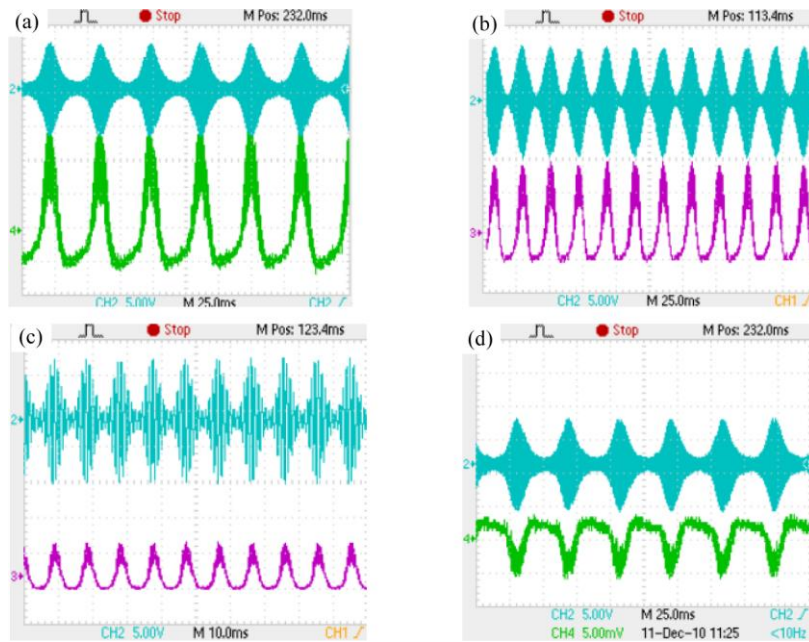


Fig. 3. H-PDLC chopper with triangle waveform is working with various duty cycles; (a) 27Hz 25ms/unit; (b) 40Hz 25ms/unit; (c) 100Hz 10ms/unit; (d) 27 Hz 25ms/unit (diffraction beam).

Figure 4 shows the results of sinusoidal waveform generating by the H-PDLC chopper. Figure 4(a)–4(c) show the working frequencies with 50Hz, 25Hz and 28Hz individually. On the oscilloscope screen, the upper yellow curve indicates the electrical signal that was applied on the H-PDLC chopper while the lower blue curves show the optical intensity modulation.

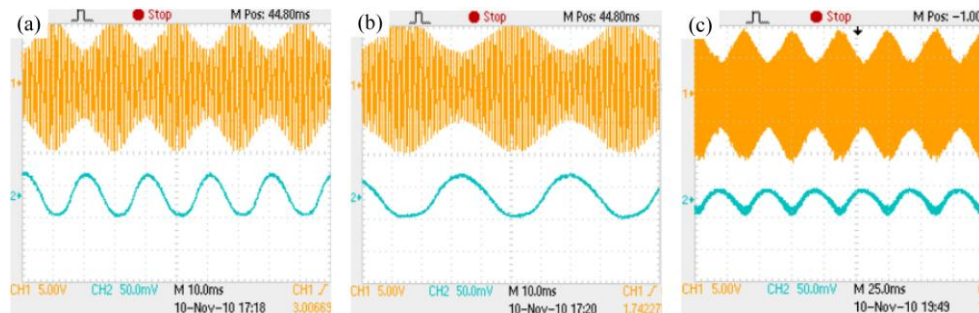


Fig. 4. H-PDLC chopper with sinusoidal waveform is working with different periods; (a) 50Hz 10ms/unit; (b) 25Hz 10ms/unit; (c) 28Hz 25ms/unit.

Figure 5 shows the experimental results of sawtooth waveform of H-PDLC chopper. Figure 5(a)–5(c) show the working frequency of H-PDLC chopper was around 10 Hz. Different electrical signals generated the different saw-tooth waveform modulation of light intensity.

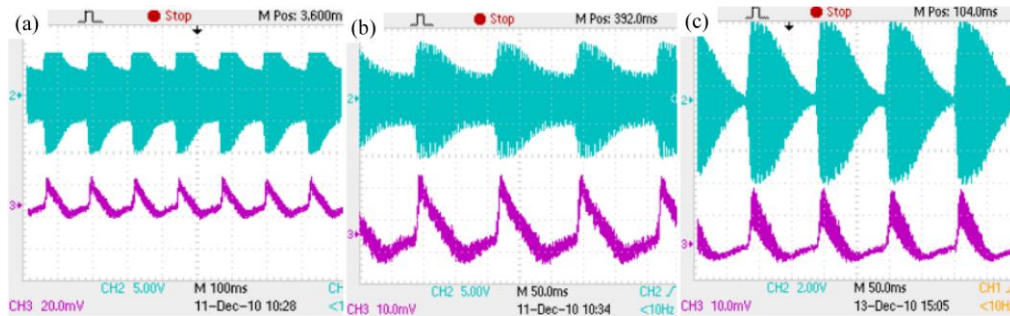


Fig. 5. Experimental results of H-PDLC chopper working with sawtooth waveform modulation; (a) 10Hz 100ms/unit; (b) 8.3Hz 50ms/unit; (c) 10Hz 50ms/unit.

Figure 6 is some of the results of integrated two-channel waveform chopper modulation. Figure 6(a) is the experimental result of 100Hz and 50 Hz square shape modulation. Figure 6(b) is the square waveform modulation at 50Hz and triangle waveform modulation at 100Hz individually. Figure 6(c) shows the 50Hz and 25Hz sinusoidal waveform modulation synchronously. Within Fig. 6(a) and 6(c), the signals in channel 1 and channel 4 indicate the electrical intensity applied on the H-PDLC gratings, while channel 2 and channel 3 represent the optical intensity modulation following with the electrical signals.

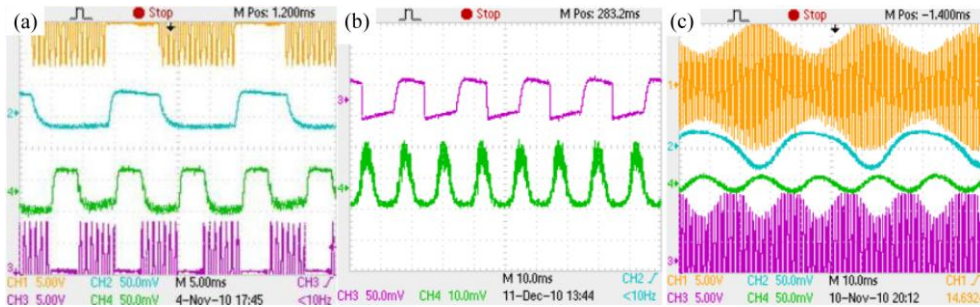


Fig. 6. Two-channel H-PDLC choppers array generate different waveform modulation; (a) 50 Hz and 100Hz square waveform; (b) 50Hz square and 100Hz triangle waveform; (c) 50Hz and 25Hz sinusoidal waveform.

4. Multichannel modulation with H-PDLC chopper array

In addition to the capability of waveform control, multichannel modulation can also be realized by using a H-PDLC chopper array. Again, for the purpose of illustration, a two-channel modulation and its application to FDMF microscopy was investigated, as illustrated in Fig. 7.

A 20 mw 405 nm laser is selected as the excitation laser source because the ultraviolet waveband can excite most of the tissue fluorophores (such as elastin, collagen, and tryptophan). First, the laser beam is expanded to a collimated circular beam shape with a diameter of 5 mm. Then, the excitation laser beam goes through a Mach-Zehnder interference optical path setup and is divided into two beams by the first beam splitter. In each beam path, two pieces of H-PDLC optical chopper are fixed with the exact Bragg incident angle, which modulate the corresponding laser beam with different frequencies, respectively. After that, those two excitation beams are recombined again, filtered by the dichromatic mirrors, coupled into the objective lens and finally focused into two points on the specimen. Then the fluorescent signals modulated with the corresponding carrying frequencies are successively collected and divided by the third beam splitter. The transmission signal is then imaged by a color CMOS camera through an imaging lens, while the reflection part is collected by a fast speed photomultiplier tube (PMT). The total intensity of the two modulated fluorescent

signals is detected by PMT and continuously fed into a computer. After the Fourier transform is done for the input signals, the frequency spectrum can be obtained, which contains two separated modulated frequencies information. After selecting the useful frequency information and doing the inversed Fourier transform calculation, the original fluorescent intensity curves varying with time can be demodulated. The unique characteristic of FDMF microscopy is the parallel detection of the multi-channel fluorescence intensity signals synchronously, which is especially useful in studying the dynamic behaviors of biological cells [1].

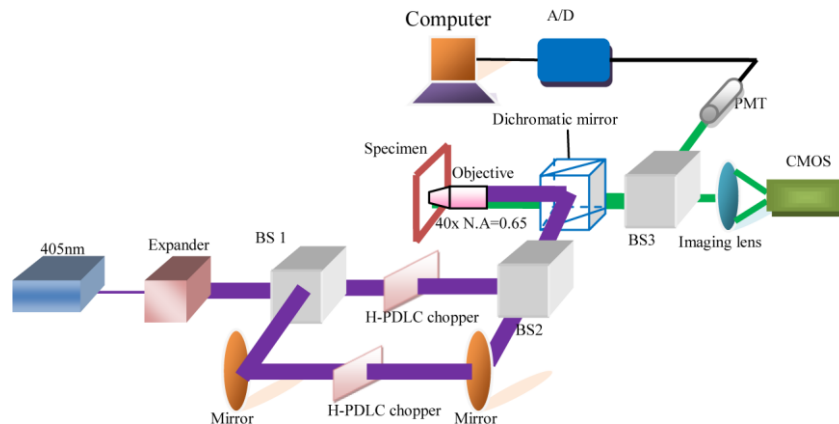


Fig. 7. An illustration of two-channel modulation in a FDMF microscopy.

The spatial resolution of this microscopy can be expressed [14] as $r_{lateral} = \frac{0.6\lambda}{N.A.}$, where λ is the emitted light wavelength, N.A. is the numerical aperture of the objective. Generally, the oil immersion objective lens ($60\times$, N.A. = 1.4) is used in fluorescent microscopy so that the weak fluorescent emission can be collected as much as possible. Suppose $\lambda = 0.5\mu m$, N.A. = 1.4, the theoretical resolution is $r_{lateral} \approx 0.2\mu m$. However, in our experimental system, we used a $40\times$ infinite objective lens (N.A. = 0.65). Therefore, the resolution is about $r_{lateral} \approx 0.46\mu m$.

5. Experimental results of FDMF microscope with H-PDLC based optical chopper

In the experiment, an adult rat hippocampus specimen was selected as the testing specimen because it played an important role in long-term memory and spatial navigation. In order to get different magnifications of the microscopy, three imaging lenses were used in the FDMF microscopy. Figures 8(a) to 8(c) are the x-y plane images using lenses with the focal lengths of 100 mm, 120 mm, and 250 mm respectively. It is shown that the longer focal length leads to a larger magnification ratio. The focal length of the infinite 40X objective lens is about 3.3 mm, therefore, the corresponding magnification ratios of FDMF are 30.3, 36.3 and 75.8 times respectively. A triple adhesive lens with a larger aperture size 120 mm and shorter focal length of 70 mm (N.A. = 0.583) was selected to collect the fluorescent signal so that the two focusing points can be observed clearly, as shown in Fig. 8(b), which are indicated by two white arrows. Again, to realize the frequency division multiplexing, an H-PDLC chopper was used to modulate the stimulating light beam so that a modulated intensity fluorescent signal could be obtained. A photomultiplier tube (PMT) (CR186 with a response time of 4 μs) was used to detect the modulated fluorescent signal.

In the experiment, the size of H-PDLC chip was 10 mm \times 20 mm, which was enough for modulating the laser beams. Two channel carrier frequencies of 50 Hz and 100 Hz were selected as the working frequencies. For the purpose of comparison, both simulated sum frequency signal and experimentally sum frequency signal were drawn in Fig. 9(a) and 9(b),

respectively. It can be seen that two curves have similar profiles, which demonstrates the correctness of our experimental result. Then we did the Fourier transform to obtain the frequency spectrum, as shown in Fig. 9(c). After the filtering and the inverse Fourier transform, the vivid variations of two-channel fluorescent emissions were obtained as shown in Fig. 9(d). It can be observed that the intensity varies in very small amplitude at two focusing spots, indicating that the fluorescent emission signals are stable since we used a dead specimen.

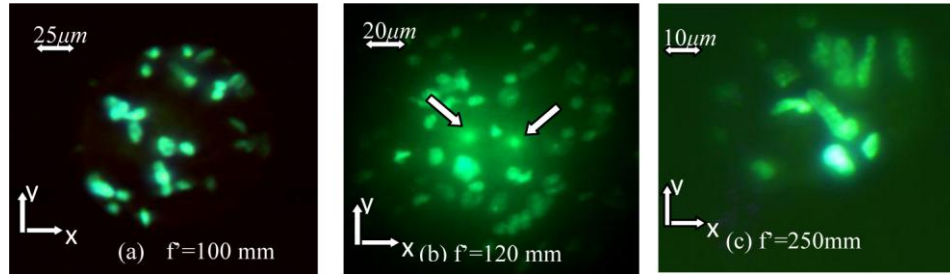


Fig. 8. The imaging pictures of rat neural cells taken by a FDMF microscope.

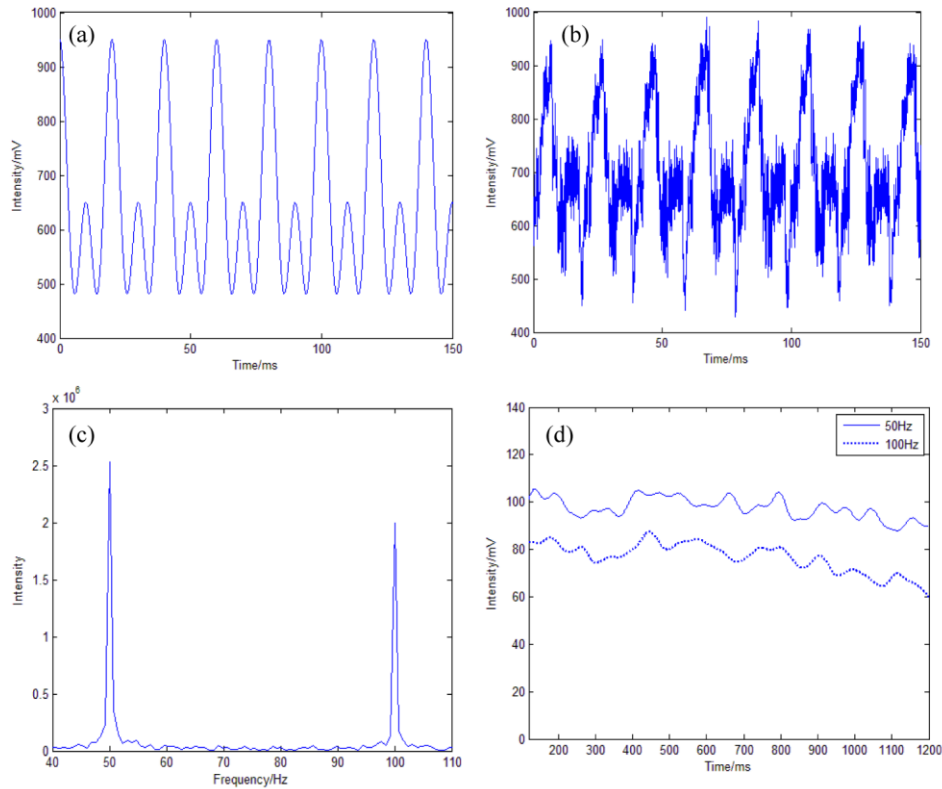


Fig. 9. The data processing of FDMF microscopy with H-PDLC chopper at 50Hz and 100 Hz; (a) Simulation of beating signal; (b) Experimental signal; (c) Sum intensity in frequency domain; (d) demodulation of fluorescence emission from two points.

5. Conclusions

In this paper, we demonstrated that waveform controllable optical choppers could be realized by employing H-PDLC gratings. Furthermore, multiple channel modulations could be achieved by employing H-PDLC gratings. Although modulation dynamic range of H-PDLC

gratings is not as good as mechanical chopper at this stage, we can still distinguish different frequency modulation channels, which is good enough for the FDMF microscopy application. We will continuously improve the diffraction efficiency and increase the number of modulation channels by taking the advantage of waveform controllable nature in the future.

Acknowledgements

The authors thank for Prof. Zhenghua Xiang from The Second Military Medical University to provide the rat neural cell specimens for the experiment. This research was supported by the National Science Foundation for Young Scholars of China (Grant No. 60801041), the Scientific Research Starting Foundation for Returned Overseas Chinese Scholars, Ministry of Education, China, and Shanghai Rising-Star Program (Grant No. 10QA1405100), and Shanghai Key Subject Construction funding (s30502).